

Title:

**STRESS-STRAIN RESPONSE OF PBX 9501
BELOW 1 GIGAPASCAL FROM EMBEDDED
MAGNETIC GAUGE DATA USING LAGRANGIAN
ANALYSIS**

Author(s):

J. J. Dick

Submitted to:

<http://lib-www.lanl.gov/la-pubs/00796355.pdf>

STRESS-STRAIN RESPONSE OF PBX 9501 BELOW 1 GIGAPASCAL FROM EMBEDDED MAGNETIC GAUGE DATA USING LAGRANGIAN ANALYSIS *

J. J. Dick

*Group DX-1, MS P952,
Los Alamos National Laboratory, Los Alamos, New Mexico 87545,*

Unsteady compressive waves were measured in the plastic-bonded, HMX-based explosive PBX 9501 using multiple, embedded, magnetic gauges that measured particle velocity. Records were obtained for impact stresses near 300 and 570 MPa. These results are analyzed using Lagrangian analysis to obtain stress-time and stress-strain curves at gauge positions.

INTRODUCTION

Embedded magnetic gauge data has been obtained on the plastic-bonded, HMX-based explosive PBX 9501 at 290 and 560 MPa. At these low stress levels the waves are not steady, therefore the Rankine-Hugoniot jump conditions are not strictly applicable to the data. However, Lagrangian analysis is applicable for analyzing the data to obtain stress and specific volume along the entire loading and unloading profile.

LAGRANGIAN ANALYSIS

The wave profiles were unsteady over the sample depth observed. However, the characteristics in h - t space for a given particle velocity were found to be straight within the precision of the data. This means that the loading wave corresponds to a nonisentropic simple wave.⁽¹⁾ The rarefaction corresponds to an isentropic simple wave. For both these cases the equations are simplified and allow direct integration of the particle velocity data to obtain stress and strain histories at positions along the wave propagation direction.

The equations governing the flow at a given gauge

position are:

$$d\sigma = \rho_0 C_\sigma du, \quad (1)$$

$$dV = -(1/\rho_0 C_u) du, \quad (2)$$

and

$$dE = -(\sigma/\rho_0 C_u) du, \quad (3)$$

(2) Here, σ is the longitudinal stress in the direction of wave propagation, ρ_0 is the initial density, u is the particle velocity, V is the specific volume, and E is the specific internal energy. C_σ and C_u are the phase velocities, the velocities of the disturbance at a given value of stress or particle velocity at that gauge position, e.g.,

$$C_u = \left. \frac{\partial h}{\partial t} \right|_u. \quad (4)$$

For the data presented here the phase velocities C_σ and C_u are equal, since the waves are simple within the data precision. The phase velocities C_u are constant, independent of time.^(1,3) Therefore, the stress and specific volume can be determined at a gauge position by integrating Eqs. 1 and 2 from the particle velocity record after the phase velocities are determined.

EXPERIMENTAL TECHNIQUE

In these experiments the impactor in the projectile was PBX 9501. By performing a symmetric impact experiment, the final particle velocity at the impact face

*Work performed under the auspices of the U. S. Department of Energy and partially supported by the Department of Defense/Office of Munitions under the Joint DoD/DOE Munitions Technology Program and the Explosives Technology Program at LANL.

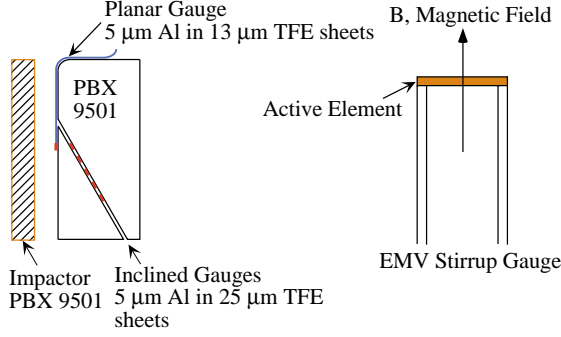


FIGURE 1. Schema of the gun impact experiment with MMV (multiple magnetic velocity) instrumentation. There are gauges at the impact face and at successive depths in the sample along the 30° cut.

was half the projectile velocity. The projectile velocity is measured to an accuracy of about 0.3%. This provides a check on the accuracy of the gauge data. A schema of the experiment is shown in Fig. 1. The experiment at 290 MPa had a planar stirrup gauge at the impact face. The particle velocity is perpendicular to the magnetic field so that the output voltage is the magnetic field times the gauge length times the particle velocity, Faraday's law.

EXPERIMENTAL RESULTS AND DISCUSSION

Particle velocity data for experiments at 290 and 560 MPa are shown in Figs. 2 and 3. For experiment 1116 at 290 MPa the final states of the first two gauges agree with half the projectile velocity within half a percent. The subsequent gauges do not attain the same final state, because the rarefaction arrives before the final state is reached. The 10 to 90% rise time of the compressive wave is $0.74 \mu\text{s}$ at the third interior gauge and $1.08 \mu\text{s}$ at the fifth gauge.⁽⁴⁾ For experiment 1049 at 560 MPa the final states are 0.4 to 3.5% higher than half the projectile velocity. The compressive wave is still unsteady, but the rise times are shorter. The 10 to 90% rise time of the compressive wave is $0.372 \mu\text{s}$ at the third interior gauge and $0.496 \mu\text{s}$ at the fifth gauge. Sample density was 1.825 g/cm^3 for experiment 1116 and 1.827 g/cm^3 for experiment 1049.

The phase velocities C_u are shown in Fig. 4 for the compression and rarefaction waves. A velocity is obtained by doing a linear least-squares fit to the h - t data at a given particle velocity; h is the gauge Lagrangian

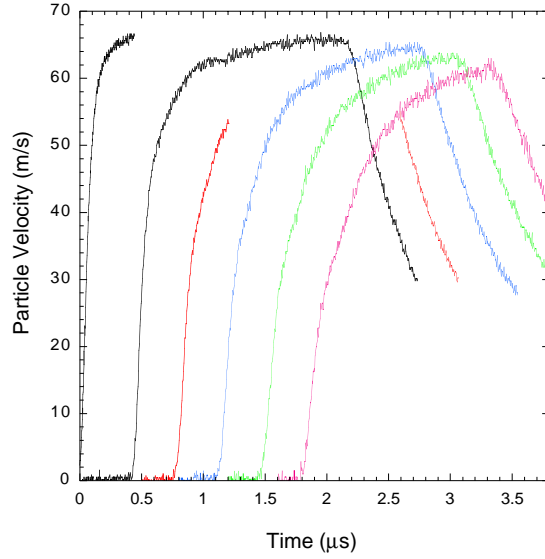


FIGURE 2. MMV gauge records in PBX 9501 at 290 MPa in a symmetric impact experiment, 1116. Gauge positions are 1.32 to 5.27 mm in from the impact face. Half the impact velocity is 66.2 m/s. The middle part of the second record at 2.32 mm was lost.

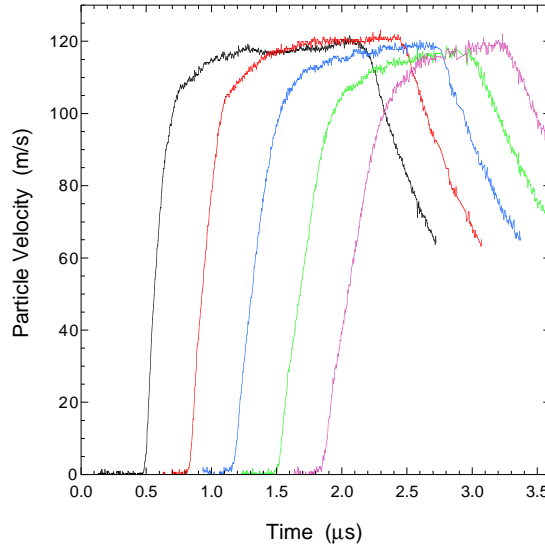


FIGURE 3. In-material particle velocity gauge records in PBX 9501 at 560 MPa in a symmetric impact experiment, 1049. Gauge positions are at 1.38 to 5.32 mm in from the impact face. Half the impact velocity is 116 m/s.

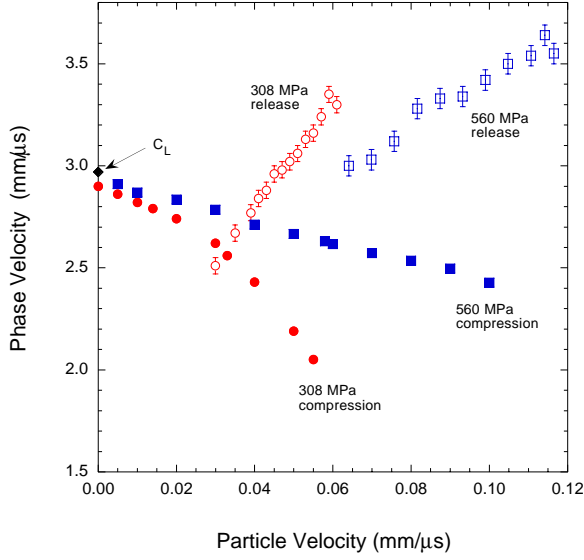


FIGURE 4. Phase velocities for compression and release in PBX 9501 at 290 and 560 MPa.

position and t is time. In general the h - t data is best fit by a straight line within the data precision. The average standard error for the phase velocities is 0.01 to 0.02 mm/μs in compression and 0.04 to 0.05 mm/μs on the release data.

At 290 MPa the C_u vs u data for the compression wave was fit in two segments corresponding to the elastic and inelastic waves. There is some dispersion in the elastic wave but less than for the inelastic wave. The intersection of the two lines corresponds to the elastic limit, a particle velocity of 0.028 mm/μs and a stress of 140 MPa. The phase velocities for compression at 560 MPa appear to follow a single line, even though a change in slope at the elastic limit is discernible at the elastic limit in the particle velocity history for the fifth gauge (Fig 3). The rarefaction velocities were fit by a single line; the profile amplitudes were normalized before these phase velocities were computed. The phase velocities for 560 MPa are in good agreement with those obtained by Olinger and Hopson at 540 MPa using three manganin gauges.⁽⁵⁾ Stress and specific volume along the profiles were obtained by integrating Eqns.1 and 2 setting $C_\sigma = C_u$. The integrations for loading and unloading are performed sequentially. The end state of the loading integration is used for the initial state for the unloading integration.

The stress-time profiles obtained for embedded

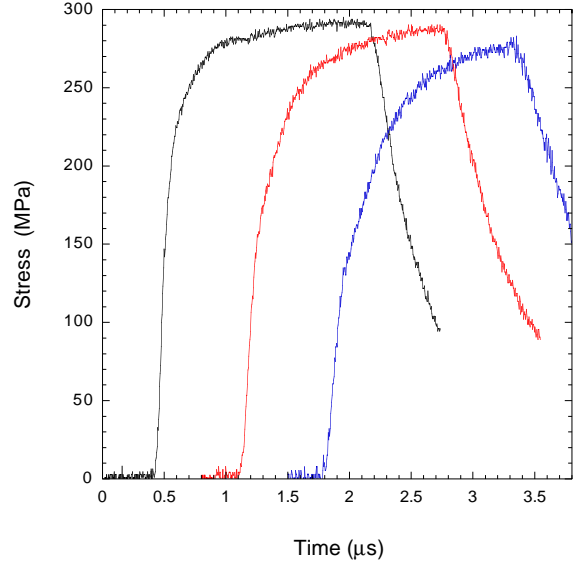


FIGURE 5. Stress-time curves in PBX 9501 at 290 MPa obtained by Lagrangian analysis. The curves are for successive depths of 1.32, 3.30, and 5.27 mm. The elastic limit at about 140 MPa is discernible on the last profile.

gauges 1, 3, and 5 in experiment 1116 are displayed in Fig. 5. The attenuation of the peak amplitude with propagation distance is apparent. Overall the σ - t profiles have wave shapes similar to the u - t profiles. This is not surprising, since for simple waves $\sigma = \sigma(u)$. In this case the phase velocity has a linear dependence on particle velocity; integration of Eq.1 results in a quadratic dependence of stress on particle velocity.

The derived stress-strain curves at 290 MPa are shown in Fig. 6. The uniaxial strain is defined as $-(V - V_0)/V_0$. Results are shown for the first, third, and fifth embedded gauges. Because the loading wave has such a long rise time, the rarefaction arrives at the third and fifth gauges before the final loading state initiated at the impact face is reached. Therefore, the stress-strain curves reach successively lower peak loading states. The net irreversible work done on the explosive after loading and unloading is proportional to the area between the the loading and unloading curves. The net irreversible work is manifested as permanent deformation and heat.

If the wave were steady, the jump conditions would apply. Then, the loading curve would be a straight line, the Rayleigh line. The states reached according to the jump conditions for the elastic state and the final state

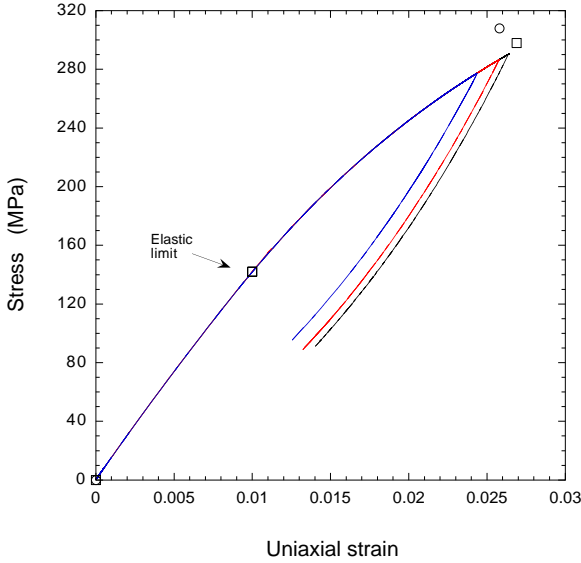


FIGURE 6. Stress-strain curve in PBX 9501 at 290 MPa obtained by Lagrangian analysis. The curves are for successive depths of 1.32, 3.30, and 5.27 mm. The peak stress is attenuated with propagation distance. The circle is the point calculated from the jump conditions assuming a single steady wave. The squares are the results assuming a two-wave structure.

are depicted for comparison to the loading curves. The elastic wave velocity was taken as equal to the phase velocity at half the elastic limit. There is not much difference between the elastic loading curve and the elastic Rayleigh line. However, the final state achieved differs markedly from the one calculated using the jump conditions, assuming a single steady wave. The jump conditions yield 308 MPa and a strain of 0.0258. By Lagrangian analysis the final stress state for the first gauge is 290 MPa, 4.5% lower than the one calculated assuming a steady wave. The strain is 0.0264. If a two-wave, Rayleigh-line analysis is performed as successive elastic and inelastic waves, the final state is 298 MPa at a strain of 0.0269. This final stress state is closer to the result for the first gauge by Lagrangian analysis, 298 MPa vs 290 MPa, a 2.8% difference.

The derived stress-strain curve at 560 MPa is shown in Fig. 7. The loading curve does not have as much curvature as at 290 MPa. All gauges reach the same final state because the rise time of the loading wave is shorter; they reach the final state before the rarefaction arrives at the gauge. Since the phase velocities are independent of gauge position h (simple waves),

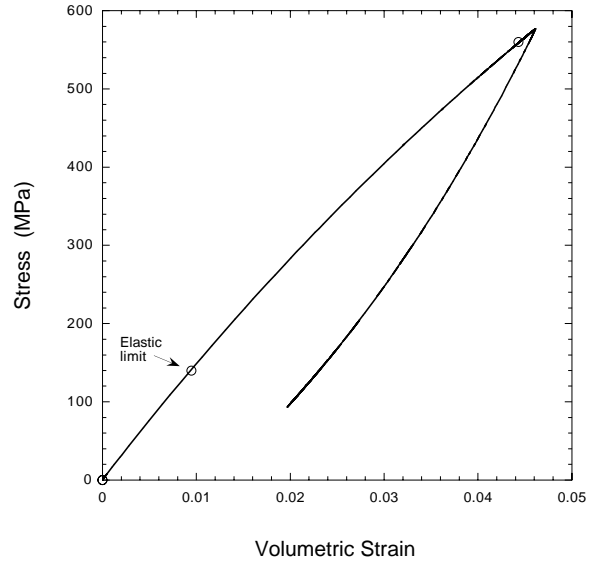


FIGURE 7. Stress-strain curve in PBX 9501 at 560 MPa obtained by Lagrangian analysis. It is compared to final states reached (circles) applying the jump conditions. The upper circle is computed assuming a single wave.

the stress-strain curve is the same for all values of h . There is better agreement between the Rayleigh line to the final state and the loading curve from Lagrangian analysis than was the case at 290 MPa. For gauge 1 the end state of the loading curve by Lagrangian analysis is 577 MPa at a strain of 0.0461 versus 560 MPa at a strain of 0.0443 by the jump conditions. The stresses differ by 3.0%. If the particle velocity data is normalized to agree with half the projectile velocity, the stress at that value is 560 MPa, in complete agreement.

ACKNOWLEDGMENTS

Helpful conversations with Chuck Forest on Lagrangian analysis are gratefully acknowledged.

REFERENCES

1. M. Cowperthwaite and R. F. Williams, *J. Appl. Phys.* **42**, 456-462 (1971).
2. R. Fowles and R. F. Williams, *J. Appl. Phys.* **41**, 360-363 (1970).
3. G. R. Fowles, in *Dynamic Response of Materials to Intense Impulsive Loading*, edited by P. C. Chou and A. K. Hopkins, (Wright Patterson AFB, Ohio, 1972), pp. 405-480.
4. J. J. Dick, A. R. Martinez, and R. S. Hixson, Los Alamos Report LA-13426-MS, April, 1998.
5. B. Olinger, and J. W. Hopson, in *Symposium H. D. P.*, (Commissariat a l'Energie Atomique, Saclay, 1978) pp. 9-19.